Atmospheric air plasma induces increased cell aggregation during the formation of Escherichia coli biofilms

SCHOLARONE™
Manuscripts
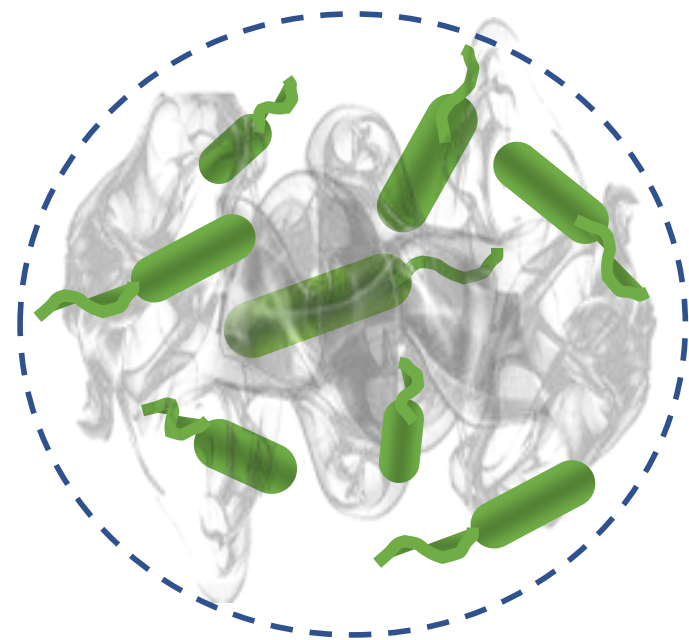
Early biofilm

Plasma
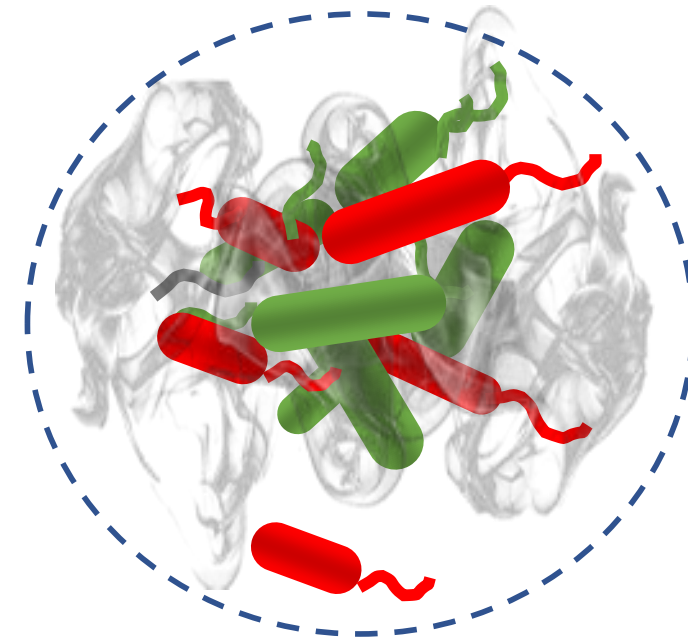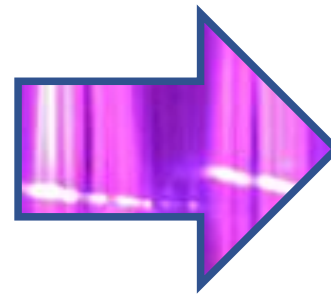
↑ cell aggregation & death

Article type: Full Paper

Atmospheric air plasma induces increased cell aggregation during the formation of Escherichia coli biofilms

Goldina Kwandou[1], Anne Mai-Prochnow[2], Stuart W. Prescott[1], Patrick T. Spicer[1] & Patrick J. Cullen[1,3]*

1 School of Chemical Engineering, UNSW, Sydney, 2052, Australia

Email: p.cullen@unsw.edu.au

2 CSIRO Manufacturing, P.O. Box 218, Lindfield, NSW 2070, Australia

3 Department of Chemical and Environmental Engineering, University of Nottingham, UK.

Keywords: atmospheric plasma; biofilms; cell agglomeration

1   **Abstract**

2   Atmospheric air plasma has previously been shown to be a novel and effective method for

3   biofilm eradication. Here we study the effects of plasma on both microbial inactivation and

4   induced structural modification for forming biofilms. New structures are created from

5   aggregates of extracellular polysaccharides and dead bacterial cells, forming a protective and

6   resilient matrix in which the remaining living cells grow and reproduce under proper growth

7   conditions. The new colonies are found to be more resilient in this state, reducing the efficacy

8   of subsequent plasma treatment. We verify that the observed effect is not caused by chemicals

9   produced by plasma reactive species, but instead by the physical processes of drying and

10   convection caused by the plasma discharge.

11

12

1. Introduction

Biofilms are colonies of microorganisms surrounded by a complex fluid matrix made predominantly of extracellular polysaccharide polymers (EPS). The EPS provides a protective barrier for bacterial colonies in a biofilm,[1] increasing the resistance of bacteria to chemical and antibiotic treatments and also reducing the efficacy of physical treatment. Biofilms can thus survive most conventional methods of eradicating more freely dispersed, or planktonic, bacteria[2]. Biofilms can form on many surfaces, including the skin of fresh fruits and vegetables, industrial pipe surfaces, in between teeth, and on medical devices.[3, 4] Due to their widespread existence and resilience, biofilms are known to be the main cause of persistent bacterial infections in hospitals,[5] contamination of foods in process environments,[6] and reduced process cleaning efficiency in manufacturing. Biofilm physical and flow properties have recently been studied as a means of understanding molecular transport through the matrix and to better enable destruction.[7, 8] New approaches are being developed to more aggressively treat biofilms during formation, for example to interfere with the attachment of these bacteria to surfaces and disturb their structure.[9]

One novel treatment currently being investigated for this purpose is atmospheric plasma, which is essentially an ionized gas that is generated at ambient temperatures and under atmospheric conditions that allows treatment of sensitive biological matter.[10, 11] Numerous recent studies have demonstrated the anti-microbial efficacy of atmospheric plasma for planktonic bacteria or cells embedded in biofilms.[12] Plasma species are reported to be capable of penetrating into the biofilm structure.[13] Plasma can inactivate biofilms with treatment times of less than 60 seconds[14] and cause a 5 log reduction in biofilm viability,[15] while longer treatments can decrease viable cells to undetected levels.[15-17] This ability of plasma to inactivate bacteria is thought to be an effect of its production of short- and long-lived reactive species[18] such as ozone and other radicals.[19] Long-lived species have been

39   shown to be effective to treat *Escherichia coli* suspensions even after a 7-day period,

40   following plasma liquid generation.[20]

41   Apart from its ability to inactivate bacteria in a biofilm, atmospheric air plasma has been

42   shown to change the overall biofilm structure by disrupting and degrading the EPS biofilm

43   components.[21] For example, separation of initially aggregated bacteria has been observed

44   during EPS degradation due to plasma treatment.[22] Plasma-induced EPS degradation causes

45   a decrease in biofilm thickness[21, 23] and volume[21] as well as an increase in its roughness and

46   porosity.[21] Plasma-treated biofilms are also known to have reduced adhesion to surfaces.[23,

47   24]

48   In model systems, monolayers of surface-deposited *Listeria innocua* responded to plasma

49   treatment by forming cell aggregates of damaged cells, into which viable cells were then

50   moved, affecting plasma inactivation kinetics.[28] Bayliss *et al*[28] suggested such sheltering of

51   cells extends the treatment time needed for bacterial inactivation and is driven by plasma gas

52   flow-induced drying and the resultant fluid shear stresses. Although the work was carried out

53   on a manually-deposited layer of cells, it likely has relevance for more developed biofilm

54   community environments as well. This work examines the effects of short duration plasma

55   treatments on young biofilm structures and how modification of those structures affects

56   bacterial resilience to subsequent plasma treatments.

57

2. Experimental Section

59   **2.1 Preparation of biofilm sample**

60   Single *E. coli* MG1655 (CSIRO Food Research Ryde Bacteriology Culture Collection)

61   colonies were inoculated in nutrient broth (1 g L^1 `Lab-Lemco' powder, 2 g L^{-1} 170 yeast

62   extract, 5 g L^{-1} peptone, 5 g L^{-1} sodium chloride, pH 7.4; Oxoid, Adelaide, Australia) and

63   grown in a shaking incubator (Bioline Global, South Australia) at 37° C and 100 rpm for 12 to

64   15 hours. The cultures contained approximately 10^9 CFU/mL which was diluted to 10^7

65   CFU/mL. From this diluted culture, 2 mL samples were transferred to a FluoroDish™ cell

66   culture dish (World Precision Instruments). These dishes were incubated at 37°C to allow

67   biofilm formation. After 24 hours, the medium was exchanged for fresh medium. The

68   biofilms were grown for a period of 48 hours total for time-dependent and liquid coverage

69   experiments or 24, 48, and 72 h for cell regrowth and multiple-treatment studies, after which

70   the medium was removed and the biofilm washed twice with phosphate buffered saline (PBS)

71   prior to treatment and analysis. Details of the regrowth studies are provided in section 2.3.

72

73   **2.2 Plasma setup**

74   The power supply used to drive the plasma discharge was an HV half bridge resonant inverter

75   circuit (PVM2000, Information Unlimited, New Hampshire, USA). The power source has a

76   maximum output voltage of 50 kV with a variable frequency of 20 kHz to 100 kHz,

77   depending on the plasma load capacitance. The plasma setup consists of a FluoroDish™ used

78   to grow the biofilm (see section 2.1) that is placed in between the electrodes of the Dielectric

79   Barrier Discharge, or DBD, consisting of a 2 mm thick poly(methyl methacrylate) dielectric

80   and a top electrode that is partially recessed within the imaging dish to reduce the discharge

81   gap to 6 mm (Figure 1a). The discharges were induced in open atmospheric air conditions.

82

83   **2.3 Plasma-biofilm treatment conditions**

84   **2.3.1   Direct treatment**

85   The growing biofilms were exposed to direct plasma treatment, Figure 1a, after 24 h or 48 h

86   of growth, while only biofilms aged 48 h were exposed to plasma-activated liquid (see section

87   2.3.2 below, Figure 1b). Plasma treatment was performed at 6 kV and ~60 kHz. The optical

88   emission spectra, OES, for the discharge were mainly in the UV region, the OES are not

89   included, the reader is referred to Lu *et al*[25] for characterisation of discharges with this power

90   source. The DBD design incorporating the dish used to grow the biofilm allows for non-

91   invasive sample preparation, which is critical for later imaging of a biofilm's structure. The

92   design also offers the added benefit of a relatively controlled discharge in terms of spatial

93   homogeneity and treatment time when compared to plasma jets. Precise control of treatment

94   time (~1s) allows the effects of short plasma treatment times on biofilm behaviour to be

95   investigated.

96   For time-dependent studies, biofilms aged 48 h were exposed to direct plasma for times

97   ranging from 0 to 60 s. The biofilm was kept wet by adding 200 μL of PBS into the dish. For

98   liquid coverage studies, different amounts of PBS were added to the cell culture dish, from

99   200 μL to 1000 μL, and biofilms aged 48 h were used. In the regrowth study, biofilms aged

100   24 h and 48 h were used and exposed to plasma for 30 s. On each day, biofilms were

101   compared to untreated controls (Table 1). After exposure to plasma, biofilms were incubated

102   again with fresh nutrient broth at 37° C. All nutrients were changed every 24 h until the final

103   day (72 h).

104

105   **2.3.2   Indirect (liquid) treatment**

106   Plasma-treated liquid was generated by treating 1 mL of PBS in the same setup as direct

107   treatment, as indicated in Figure 1B. After treatment, 200 μL of the liquid was removed from

108   the dish and transferred to another dish containing the biofilm, and subsequently incubated for

109   1 hour prior to imaging. Commercial hydrogen peroxide (Chem-Supply Pty Ltd, South

110   Australia, Australia) was employed for comparison to the plasma-treated liquid via addition to

111   PBS. Similarly, 200 μL of these peroxide-PBS solutions were also incubated for 1 hour with

112   the biofilm prior to imaging.

113

2.4 Confocal Laser Scanning Microscopy (CLSM)

115 Before imaging, the biofilm was dyed with Live/Dead BacLight™ Bacterial Viability Kits

116 (Thermo Fisher Scientific, Victoria, Australia), which contains SYTO9 and Propidium Iodide

117 (PI), following supplier's instructions. The dishes were then incubated in the dark for about

118 15 mins before imaging. Biofilm imaging was performed on a Leica TCS SP5 STED inverted

119 confocal microscope with oil objective 63×, NA 1.4. The lasers used for imaging were at 488

120 nm for SYTO9 and 498 nm for PI.

121

2.5 Image analysis

123 All images were analysed using Image-J.[26] Green and red channels from CLSM data were

124 separated and then analysed individually to calculate biofilm coverage area. From the

125 literature it is known the approximate size of one *E. coli* cell is 1μm x 3μm.[27] Assuming the

126 cells are perfectly oval, the area of one *E. coli* cell is 2.35 μm^2. Hence, any number that is less

127 than this value is disregarded in the calculation. The percentage of red cells was calculated

128 from total area covered by red cells divided by the total area covered by both green and red

129 cells. Each data set contains at least six fields of view that are used for data quantification.

130

2.6 Hydrogen peroxide (H_2O_2) measurement

132 Quantification of H_2O_2 concentration in the plasma liquid was performed following the

133 protocol of Pick and Keisari.[28] Briefly, 5 g of horseradish peroxidase Type II (Sigma Aldrich,

134 Sydney, Australia) powder was dissolved in 0.05 M phosphate buffer. Phenol red dye is used

135 to detect colour change due to the presence of H_2O_2, using a concentration of 0.28 mM.

136 Standard curves were then prepared by measuring spectra of milli-Q water containing various

137 concentrations of H_2O_2 from 0-60 μM. The solution was taken out of the dish, transferred into

138   a small glass vial, and incubated for 1 hour before spectra measurement. Just before spectra

139   measurement, 10 μL of the horseradish peroxidase solution and 10 μL of the phenol red

140   solution were added into the standard samples and plasma-treated liquid. These vials were

141   then incubated again at 25° C for 5 mins. After incubation, NaOH was added to the solution

142   to change its color from orange to purple and keep the colour stable.[28] Spectra of samples at

143   610 nm were then recorded using a UV-VIS spectrophotometer (Shimadzu Corporation,

144   Kyoto, Japan).

145

146

147   **3. Results & Discussion**

148   **3.1 The effect of plasma treatment on biofilm structure**

149   Plasma treatment has been reported previously to destabilize biofilm structures.[21] Here we

150   use an *Escherichia coli* biofilm that is in a younger state than the previously studied biofilms

151   of *Pseudomonas aeruginosa* or *Staphylococcus aureus*.[21] During this early stage of biofilm

152   development, no microcolonies have been formed. Figure 2a shows the microscopic initial

153   state of these young biofilms, with green live cells visible throughout the field of view at t = 0

154   s. Figure 2a also shows micrographs of the biofilm after different plasma exposure times,

155   enabling tracking of the kinetic progression of cell death by following the increase in red, or

156   dead, cells and the survival of the green, or living, cells and the formation of cell clumps.

157   These effects are contrary to those reported by Ferrell *et al*, [21] with plasma treatment

158   inducing aggregation and forming a new structure rather than structure breakdown. This

159   plasma-induced structural re-arrangement has been observed previously in surface-deposited

160   planktonic bacteria.[29]

161   Figure 2a shows that cell aggregation occurred for all treatment times tested. However,

162   quantitative analysis via cell imaging revealed that there was only a slight increase in the

163   percentage of larger aggregates (>10 μm^2) as a function of treatment time (Figure 2b). An

164   aggregate area cutoff value of 10 μm^2 was chosen to differentiate aggregates from cells in

165   sufficient proximity to be classified as an aggregate. An increase was only observed between

166   the untreated and the shortest treatment time of 10 s (around 20% increase), indicating that

167   cell aggregation occurs rapidly and is not significantly governed by treatment time.

168   Figure 2b shows that although plasma treatment causes cell aggregation, it also inactivates

169   bacterial cells in the biofilm. This behaviour has been observed in many studies that study the

170   effect of treatment on bacterial viability.[15-17] However, for the current system, it is found that

171   after 40 s the number of dead cells reaches a plateau of 40%, Figure 2b. This indicates that

172   there is a limit to the number of bacteria that can be killed with plasma treatment, perhaps

173   because aggregation offers some form of protection.

174   Of particular interest is that the aggregation of the cells and the mortality effects of the plasma

175   appear to both plateau, although on different time scales, after 40 s for cell viability and after

176   10 s for cell aggregation (Figure 2b).

177   The biofilms used in this study are considered mature once they are 48 h old, but we also

178   examined the effects of biofilm age on aggregation and mortality response to plasma

179   treatment. This is because the amount of EPS increases with biofilm age, and it may play a

180   role in protecting cells from plasma and aggregation induced by plasma.

181   When subjected to the same plasma treatment for 30 s, both biofilms aged 24 h and 48 h form

182   aggregates (Figure 3a). The percentage of big aggregates formed in these two samples is quite

183   similar, although the actual percentage of bigger clumps is slightly higher for the treated

184   younger biofilm. The older biofilm is expected to have more EPS, which might explain why

185   there is a slight discrepancy between the two values. Aggregation requires both attractive

186   interactions between cells and sufficient mobility to bring cells together for collision. The

187   cells in the older biofilm might move less than the cells in younger ones, resulting in the

188   current observation.

189   Figure 3 also shows that older biofilms have increased resistance to plasma treatment. In

190   Figure 3c, the percentage of dead cells after treatment increased compared to the control. For

191   biofilms aged 24 h, the percentage of dead cells increases from around 2% to 40% upon

192   treatment. The efficacy of plasma decreases with increasing age of biofilm, as the percentage

193   of dead cells only increases from 2% to 25% upon treatment, about half of the impact seen for

194   biofilms aged 24 h.

195

196   **3.2 Regrowth of surviving bacteria**

197

198   When plasma treatment does not inactivate all bacterial cells in a biofilm, the surviving cells

199   may be able to grow and reproduce when given sufficient nutrients. Under these

200   circumstances, we are interested in how these bacterial cells regrow in their restructured

201   environment. To answer this question, both younger and more mature biofilms were exposed

202   to plasma treatment and then regrown, until the biofilm reached an age of 72 h, before being

203   imaged.

204   Biofilms that have been treated at least once after regrowth have distinct structures when

205   compared to previously untreated biofilms with the same treatment. Figure 4a indicates that

206   biofilms treated at least once during their growth have clearly aggregated structures compared

207   to untreated biofilms that retain a fully dispersed structure. Indeed, after plasma treatment of

208   biofilms either 24 h or 48 h old, bacteria keep growing in the aggregates instead of growing

209   separately as in the untreated samples. This indicates that the surviving bacteria are able to

210   reproduce and grow in this newly formed structure.

211   Yet, these aggregated structures that occur after treatment at 24 h and 48 h, or treated twice at

212   24 h 48 h old, are hardly distinguishable from each other. Quantitative analysis on the

213   aggregates (Figure 4b) reveals that biofilms treated at 24 h have a higher percentage of

214   aggregates larger than 10μm^2 than a biofilm treated at 48 h or treated at 24 h & 48 h. This

215   may be due to fact that biofilms treated at 24 h have more time to expand the size of their

216   colonies as longer growth time increases cell cluster size.[30]

217   In addition, as seen from Figure 4a, a plasma-treated biofilm consists of only living cells.

218   Analysis shows that despite 30 s of plasma treatment causing cell death of a significant

219   proportion of cells (Figure 4c), only a very small number (< 10 %) of dead cells could be

220   detected after biofilm re-growth. However, it is likely that some dead cells are hidden within

221   the new structure. However, the percentage of these red cells is still quite low, less than 10%,

222   which is not significant.

223

224   **3.3 The effect of plasma-induced biofilm structure on subsequent treatment**

225

226

227   In section 3.2, it was found that after plasma treatment, bacteria in a biofilm can utilize the

228   new structure to reproduce and grow. In previous work by Ferrell *et al*,[21] a mature biofilm

229   with large aggregates was shown to change structure by increasing the porosity of the biofilm

230   structure. In this kind of mature biofilm, the high amount of EPS should prevent the

231   aggregation of bacteria as this EPS provides elastic resistance to deformation by flow. The

232   plasma-treated biofilm has a structure more similar to the mature biofilm used by Ferrell *et*

233   *al*.[21] It is interesting to know if this plasma-mediated structure has a similar behaviour to a

234   mature biofilm.

235   To answer this, biofilms were exposed to plasma after 24 h of growth. This sample is

236   incubated again for another 24 h before exposing this to the second plasma treatment. Figure

237   5a shows that clumping is still apparent in this system. However, quantitative analysis shows

238   that the relative amount of aggregates decreases after the second plasma treatment instead of

239   increasing. This observation agrees with Ferrell *et al.'s*[21] work. This also indicates that after

240   a certain point, aggregation is not possible anymore as biofilms might produce enough EPS to

241   resist deformation by plasma. Another explanation is that subsequent plasma treatments can

242   destroy structures formed by previous treatments.

243   Interestingly, Figure 5a also indicates that biofilms that have been previously treated mainly

244   consist of live cells. This result is unexpected as when the sample is treated twice, it is likely

245   that the percentage of red cells should be higher compared to 24 h or 48 h old biofilms. As

246   can be seen from Figure 5c, the percentage of dead cells in the sample treated both at 24 h and

247   48 h is about 5% which is much lower than the percentage of cells inactivated by single

248   treatment when they were 24 h (by 6 times) or 48 h old (by 4 times). This suggests that the

249   bacteria developed resistance after the first treatment that reduced efficacy of the second

250   treatment, consistent with other reports of resistant colonies induced by plasma treatment.[16,

251   31]

252

3.4 The effect of plasma chemicals on biofilm structure

254   In the literature, the death of bacterial cells induced by plasma is usually associated with the

255   presence of reactive species produced by plasma treatment. It is plausible that such chemicals

256   could also cause clumping, as bacteria are known to respond to chemicals present via

257   chemotaxis. Chemotaxis is the phenomenon by which motile cells move towards or away

258   from a chemical by altering their swimming pattern. Bacteria such as *E. coli* have several

259   flagella per cell which facilitate some directional control over their motion to either find

260   favourable locations with high concentrations of attractants or to avoid repellents,[32] such as

261   chemicals produced by plasma. Although chemotaxis traditionally is known only for motile

262   cells, recent finding shows that chemotaxis might also occur in surface-attached cells.[33]

263

264   One of the chemicals often found in atmospheric plasma-treated liquid is H_2O_2.[19, 34] For this

265   work only H_2O_2 is measured, for a more comprehensive species diagnostic of PAW using this

266   power source, the reader is referred to our recent publications.[25, 35] Figure 6b indicates that

267   the concentration of H_2O_2 in the liquid increases with increasing treatment time. This

268   behaviour has been seen in plasma-treated water previously, where initially the concentration

269   of peroxide increases linearly before reaching a plateau.[25]

270   If the aggregation observed previously is related to the presence of chemicals produced by

271   plasma reactive species, we should be able to induce such aggregation by adding commercial

272   H_2O_2, or plasma-treated water, to the biofilms and comparing the result to plasma-treated

273   biofilms. The concentration of H_2O_2 added to the liquid is the same as the concentration of

274   H_2O_2 in water treated in plasma for 60 s, which is 30 µM.

275

276   Figure 7a shows that biofilms that were exposed to plasma-treated liquid or 30 µM peroxide

277   solutions are similar to the control. Data analysis (Figure 7b) reveals that there are actually

278   changes in clumping after addition of peroxide or incubation with plasma water compared to

279   control. Figure 7b also shows that compared to peroxide only, plasma water increases the

280   extent of clumping by 2 times (from 3% to 6%), which might suggest that presence of other

281   chemicals that also give rise to cell clumping. However, the change in clumping caused by

282   chemicals (~6%) is not as much as the clumping caused by direct treatment (~20%). This

283   suggests that aggregate formation might be slightly affected by chemicals present in plasma-

284   treated water, but it is not the main mechanism. Movement of bacteria is also required for

285   aggregation and is likely controlled by plasma discharge-induced flow.[28]

286   Additionally, the use of hydrogen peroxide and plasma liquid here does not cause significant

287   cell death. As shown in Figure 7b, the percentage of cells killed by treatment is very small,

288   less than 2%. These values are similar to the levels in untreated biofilms. This means there is

289   very little effect of plasma-treated water, which is not in agreement with literature as plasma-

290   treated liquid has been shown to inactivate bacteria in biofilms.[36, 37] But, literature[38, 39] has

291   indicated that in order for plasma-treated liquid to be effective in inactivating bacteria,

292   acidified conditions are required. Naïtali *et al*[38] showed that in plasma-treated water, a

293   bacterial population was reduced from 8 log CFU to 2 log CFU. However, the effect was

294   diminished for buffered plasma liquid where only a minimal reduction was observed. As all

295   experiments here use a buffer solution, PBS, the pH of the solution is not expected to change

296   and become acidified.

297

298   **3.5 Dilution effect on biofilm structure**

299

300   As mentioned before, the formation of ring structure has been observed in surface deposited

301   bacteria, which is said due to drying by plasma jet.[29] This means that there is high possibility

302   that the structure here is also caused by drying. To understand better the drying by our plasma

303   system, we measured how much water removed when exposed to plasma.

304   Table 2 shows that for 30s treatment time, plasma treatment removes between 0.04-0.06 g

305   water from the system by evaporation regardless of the starting amount of water. From this

306   result, it appears that there is a maximum amount of water that can be removed by plasma for

307   the same treatment time. On the other hand, Table 2 also indicates that the percentage of

308   water removed changes depending on the amount of initial liquid covering biofilm. In this

309   case, the maximum of water removed is 32.9% for a biofilm covered with 200 μL of water

310   (Table 2). Additionally, this suggests that after plasma treatment for 30s, biofilms will not

311   completely dry out. Thus, from this observation it is therefore likely that larger volumes of

312   water could reduce the drying and convective effects of plasma treatment in a specified

313   treatment time. Interestingly, we have observed that biofilms that were completely dried in an

314   oven overnight have a similar structure to these plasma-treated samples (data not shown).

315   The above experiments were repeated with biofilms present in varying amounts of water and

316   a constant plasma exposure time of 30s. Figure 8 summarizes the results obtained from this

317   experiment. It is clear that biofilms can aggregate in liquid volumes up to 600 μl. However,

318   when biofilms are in larger liquid volumes (>600 μl) no aggregation was observed,

319   presumably due to a protective effect from the liquid against drying.

320   Figure 8b also indicates that aggregation and cell death was steadily reduced with increasing

321   amounts of liquid. Increasing the amount of water by 200 μL lowers the percentage of dead

322   cells and also reduces the extent of clumping by around 10%. For biofilms that are covered by

323   800 μL and 1000 μL, the clumping effect and amount of cell death is very small. This

324   confirms the hypothesis that extra liquid protects biofilms during plasma treatment and

325   reduces the drying effect imposed by plasma discharge. Although plasma drying is not

326   mentioned much in the literature as a mechanism of plasma inactivation, it is an important

327   factor governing cell death. Due to this, the effect of plasma drying during treatment has to be

328   taken into account when treating bacteria or biofilms, as this effect is apparent even when

329   biofilms are treated for very short times.

330

331

3.6 Explanation of structure formation

333   Our results from the previous section indicate that the structure generated by plasma treatment

334   is mainly due to a drying effect. There is a difference in the convection produced by plasma

335   and standard oven, as Figure 10a & b indicates treatment with a conventional oven at 50°C

336   (average temperature of cold plasma) for the same time scale (30 s or 60 s) could not cause

337   the same effect of aggregation. In addition, as can be seen from Figure 10c, even prolonged

338   dehydration for 90s using the oven could not cause the same clumping effect as plasma

339   treatment, although there is idication of some cell death.

340   The circular pattern observed in Figure 9a resembles Benard cells, hexagonally-ordered

341   structures that spontaneously form in fluids with a convection flow during heating or

342   evaporation.[40] The length scale of this structure is on the order of μm and is similar to

343   structures formed by surface-deposited bacteria,[29] as depicted in Figure 9c.

344   Deegan *et al* [41] showed that various patterns can be created by changing the conditions of

345   evaporation. Apart from the formation of Benard cells where the deposit forms a ring, Deegan

346   *et al* [41] also observed the formation of compact structures as we observed in our biofilm

347   (Figure 9b). As biofilms are known to have a heterogeneous spatial structure, the plasma jets

348   are also generally heterogeneous in their effects on targets, resulting in the two distinct

349   structures observed. Fischer[42] reported the formation of such ring structures only occurs

350   when there is outward flow to replenish liquid evaporating from the edges.

351   The fact that there is a limit of maximum liquid coverage of biofilms for significant

352   convective effects may be related to the conditions required for Benard cell formation in thin

353   films, namely that the thickness be less than 1 mm. [43] In our experiments, water mainly

354   covered the inner area of the FluoroDish™, which has an overall diameter of 23.5mm.

355   Assuming that liquid covers the inner area uniformly and the area is in cylindrical shape, the

356   volume of liquid added to each system allows us to calculate the height of liquid covering the

357   biofilm. It was found that only biofilm containing 200 μL and 400 μL liquid is covered by

358   water layer which is less than 1 mm thick. This agrees with the finding that aggregation of

359   cells is more apparent in those samples.

360   Drying of 200 μL water for 30 s by oven only removed 1.6 ±0.25% water, which is around 20

361   times lower than drying the same amount of water by plasma (Table 2). Probstein[43] also

362   indicates that for thin films around 0.5-1 mm deep, the cell spacing should be around three

363   times the liquid depth. The difference between the two might relate to the different rate of

364   drying of plasma, oven or natural convection. In addition, the fact that biofilms have

365   polymeric gels that encapsulate them, might reduce the rate of bacterial cell migration during

366   drying, hence smaller size structures were observed.

367

368   4. Conclusions

369   Plasma can be an effective treatment for biofilm eradication. However, this study found that

370   plasma can also induce new structures within the biofilm, which can persist after treatment

371   during regrowth. This phenomenon was evident for both young and more mature biofilms.

372   Once such structures form, subsequent treatments are less effective in terms of efficacy, likely

373   due to the surviving bacteria becoming increasingly resistant to plasma. The structures

374   induced for the biofilms tested are similar to those observed previously for plasma-treated

375   surface-deposited bacteria.[29] The observed structures are reminiscent of Benard cells, whose

376   main mechanism of formation is convection. Secondary plasma species formed in the liquid

377   phase were not found to induce the formation of such structures.

Table 1. Design of regrowth experiment where U indicates untreated and T treated samples

Biofilm age (h)	Control	Treatment		
24	U	T24		
48	U	T48	T24+48	
72	U	T24+48	T 24	T48

Table 2. The amount of water removed by plasma treatment

Amount of water in dish (µL)	Amount of water removed (g)	Percentage of water removed (%)
200	0.064 ± 0.024	32.9±2.7
400	0.053 ± 0.007	13.3±1.7
600	0.044 ± 0.011	7.4±1.9
800	0.060 ± 0.019	7.5± 2.3
1000	0.051 ± 0.013	5.1 ± 1.3

References

1. H.-C. Flemming and J. Wingender, *Nat Rev Micro*, **2010**. *8*(9): p. 623-633.
2. T.-F.C. Mah and G.A. O'Toole, *Curr Trends Microbiol.*, **2001**. *9*(1): p. 34-39.
3. R.M. Donlan, *Emerg. Infect. Dis.*, **2001**. *7*(2): p. 277.
4. R.M. Donlan, *Emerg. Infect. Dis.*, **2002**. *8*(9): p. 881-890.
5. L. Hall-Stoodley, J.W. Costerton, and P. Stoodley, *Nat Rev Micro*, **2004**. *2*(2): p. 95-108.
6. S. Srey, I.K. Jahid, and S.-D. Ha, *Food Control*, **2013**. *31*(2): p. 572-585.
7. A. Birjiniuk, N. Billings, E. Nance, J. Hanes, K. Ribbeck, and P.S. Doyle, *New J. Phys.*, **2014**. *16*(8): p. 085014.
8. E.J. Stewart, M. Ganesan, J.G. Younger, and M.J. Solomon, *Sci. Rep.*, **2015**. *5*: p. 13081.
9. M. Chen, Q. Yu, and H. Sun, *Int. J. Mol. Sci.*, **2013**. *14*(9).
10. N.N. Misra, B.K. Tiwari, K.S.M.S. Raghavarao, and P.J. Cullen, *Food Eng Rev*, **2011**. *3*(3): p. 159-170.
11. C. Tendero, C. Tixier, P. Tristant, J. Desmaison, and P. Leprince, *Spectrochim. Acta B*, **2006**. *61*(1): p. 2-30.
12. S.G. Joshi, M. Paff, G. Friedman, G. Fridman, A. Fridman, and A.D. Brooks, *Am J Infect Control*, **2010**. *38*(4): p. 293-301.
13. Z. Xiong, T. Du, X. Lu, Y. Cao, and Y. Pan, *Appl. Phys. Lett.*, **2011**. *98*(22): p. 221503.
14. M.Y. Alkawareek, Q.T. Algwari, G. Laverty, S.P. Gorman, W.G. Graham, D. O'Connell, and B.F. Gilmore, *PLoS ONE*, **2012**. *7*(8): p. e44289.
15. D. Ziuzina, S. Patil, P.J. Cullen, D. Boehm, and P. Bourke, *Plasma Medicine*, **2014**. *4*(1-4): p. 137-152.
16. A. Mai-Prochnow, M. Bradbury, K. Ostrikov, and A.B. Murphy, *PLoS ONE*, **2015**. *10*(6): p. e0130373.
17. D. Ziuzina, D. Boehm, S. Patil, P.J. Cullen, and P. Bourke, *PLoS ONE*, **2015**. *10*(9): p. e0138209.
18. D.X. Liu, Z.C. Liu, C. Chen, A.J. Yang, D. Li, M.Z. Rong, H.L. Chen, and M.G. Kong, *Sci. Rep.*, **2016**. *6*: p. 23737.
19. L.F. Gaunt, C.B. Beggs, and G.E. Georghiou, *IEEE Trans. Plasma Sci.*, **2006**. *34*(4): p. 1257-1269.
20. J.T. Matthew, J.P. Matthew, K. Sharmin, H. Pritha, S. Yukinori, S.C. Douglas, and B.G. David, *J. Phys. D*, **2011**. *44*(47): p. 472001.
21. J.R. Ferrell, F. Shen, S.F. Grey, and C.J. Woolverton, *Biofouling*, **2013**. *29*(5): p. 585-599.
22. M.S.I. Khan, E.-J. Lee, and Y.-J. Kim, *Sci. Rep.*, **2016**. *6*: p. 37072.
23. A.J. Zelaya, G. Stough, N. Rad, K. Vandervoort, and G. Brelles-Mariño, *IEEE Trans. Plasma Sci.*, **2010**. *38*(12): p. 3398-3403.
24. K.G. Vandervoort and G. Brelles-Mariño, *PLoS ONE*, **2014**. *9*(10): p. e108512.
25. P. Lu, D. Boehm, P. Bourke, and P.J. Cullen, *Plasma Process Polym.*, **2017**: p. e1600207-n/a.
26. C.A. Schneider, W.S. Rasband, and K.W. Eliceiri, *Nat Meth*, **2012**. *9*(7): p. 671-675.
27. G. Reshes, S. Vanounou, I. Fishov, and M. Feingold, *Biophys. J.*, **2008**. *94*(1): p. 251-264.
28. E. Pick and Y. Keisari, *J Immunol Methods*, **1980**. *38*(1): p. 161-170.
29. D.L. Bayliss, J.L. Walsh, F. Iza, G. Shama, J. Holah, and M.G. Kong, *Plasma Process Polym.*, **2012**. *9*(6): p. 597-611.
30. H. Beyenal, Z. Lewandowski, and G. Harkin, *Biofouling*, **2004**. *20*(1): p. 1-23.
31. R.E.J. Sladek, S.K. Filoche, C.H. Sissons, and E. Stoffels, *Lett Appl Microbiol*, **2007**. *45*(3): p. 318-323.
32. J. Adler, *Science*, **1966**. *153*(3737): p. 708-716.
33. N.M. Oliveira, K.R. Foster, and W.M. Durham, *Proc. Natl. Acad. Sci. U.S.A.*, **2016**. *113*(23): p. 6532-6537.
34. K. Oehmigen, J. Winter, M. Hähnel, C. Wilke, R. Brandenburg, K.-D. Weltmann, and T. von Woedtke, *Plasma Process Polym.*, **2011**. *8*(10): p. 904-913.
35. P. Lu, D. Boehm, P. Cullen, and P. Bourke, *Appl. Phys. Lett.*, **2017**. *110*(26): p. 264102.

36. U. Ercan, Joshi, S. , Yost, A. , Gogotsi, N. , O'Toole, S. , Paff, M. , Melchior, E. and Joshi, S., *Adv Microbiol.*, **2014**. *4*: p. 1188-1196.

37. G. Kamgang-Youbi, J.M. Herry, T. Meylheuc, J.L. Brisset, M.N. Bellon-Fontaine, A. Doubla, and M. Naïtali, *Lett Appl Microbiol*, **2009**. *48*(1): p. 13-18.

38. M. Naïtali, G. Kamgang-Youbi, J.-M. Herry, M.-N. Bellon-Fontaine, and J.-L. Brisset, *Appl. Environ. Microbiol.*, **2010**. *76*(22): p. 7662-7664.

39. K. Oehmigen, M. Hähnel, R. Brandenburg, C. Wilke, K.D. Weltmann, and T. von Woedtke, *Plasma Process Polym.*, **2010**. *7*(3-4): p. 250-257.

40. L. Rayleigh, *Philos. Mag.*, **1916**. *32*(192): p. 529-546.

41. R.D. Deegan, O. Bakajin, T.F. Dupont, G. Huber, S.R. Nagel, and T.A. Witten, *Phys Rev E*, **2000**. *62*(1): p. 756-765.

42. B.J. Fischer, *Langmuir*, **2002**. *18*(1): p. 60-67.

43. R.F. Probstein, *Surface Tension*, in *Physicochemical Hydrodynamics*. **1993**, Wiley. p. 267-318.
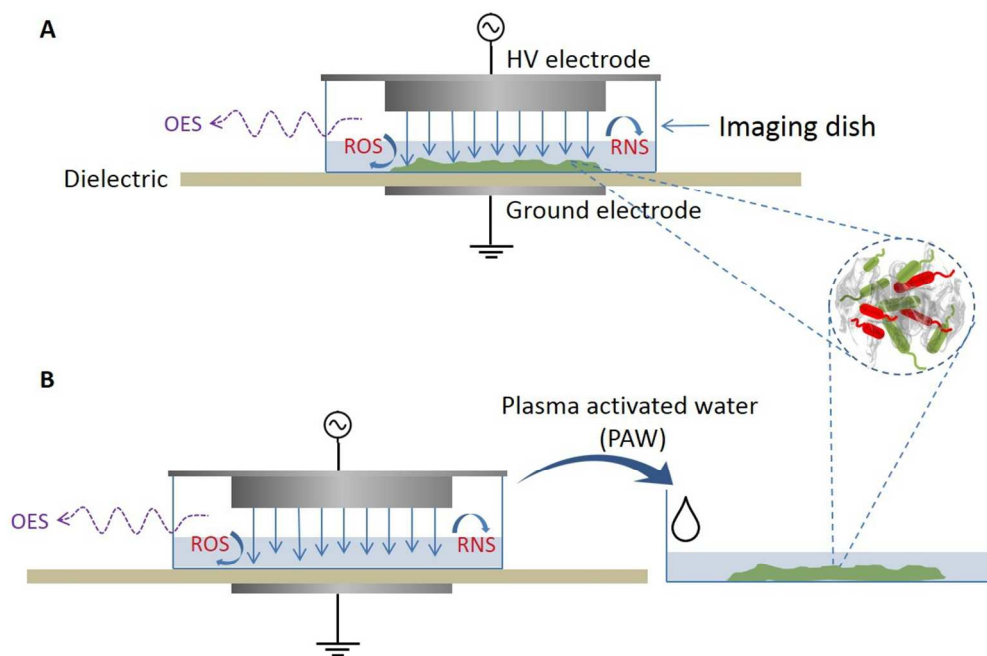
Figure 1. a) DBD design incorporating the glass bottom imaging dish containing the growing biofilm within the discharge gap, b) Schematic of air discharge in contact with liquid and addition of PAL to growing biofilm.

206x134mm (150 x 150 DPI)
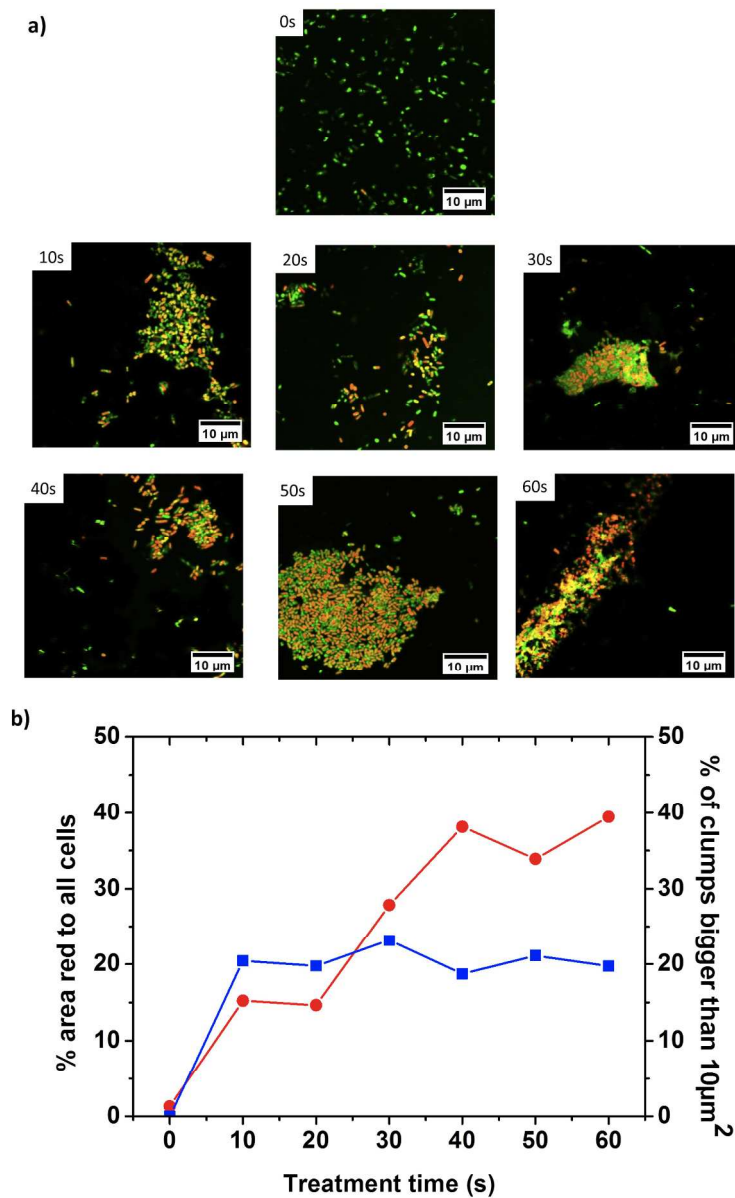
Figure 2. Effect of treatment time on biofilm structure a) Confocal images of biofilm structure before and after plasma treatment, b) quantification of dead cells (symbol ●) and cell clumps larger than 20µm2 (symbol)

293x467mm (300 x 300 DPI)
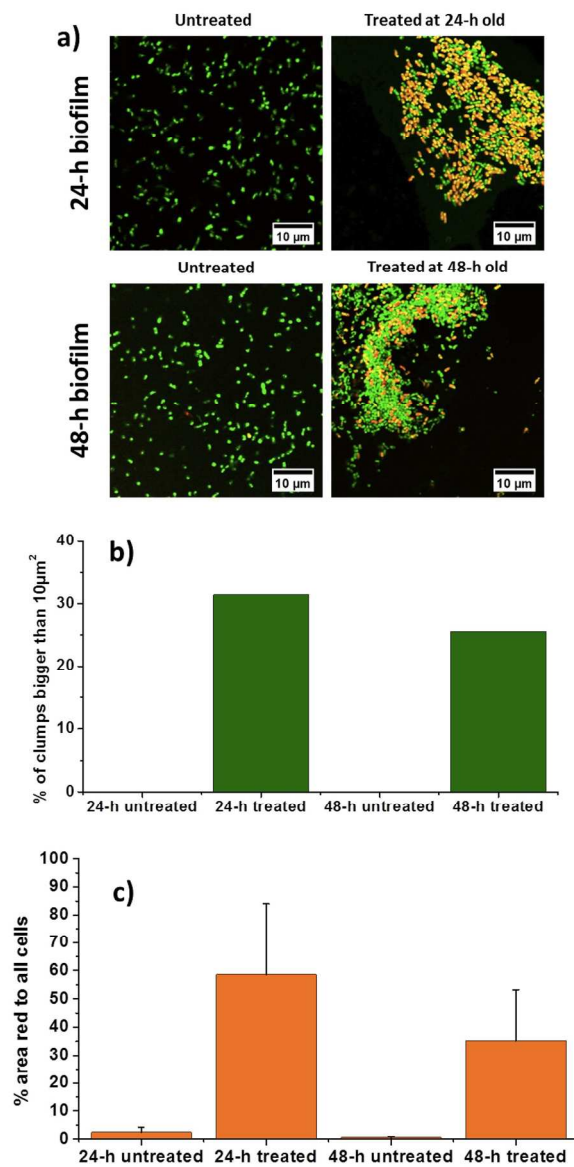
Figure 3. Effect of biofilm maturity on plasma clumping a) confocal images of 24-h and 48-h of untreated and plasma treated biofilm, b) percentage of clumps bigger than 20µm2, c) quantification of red cells.

172x281mm (300 x 300 DPI)
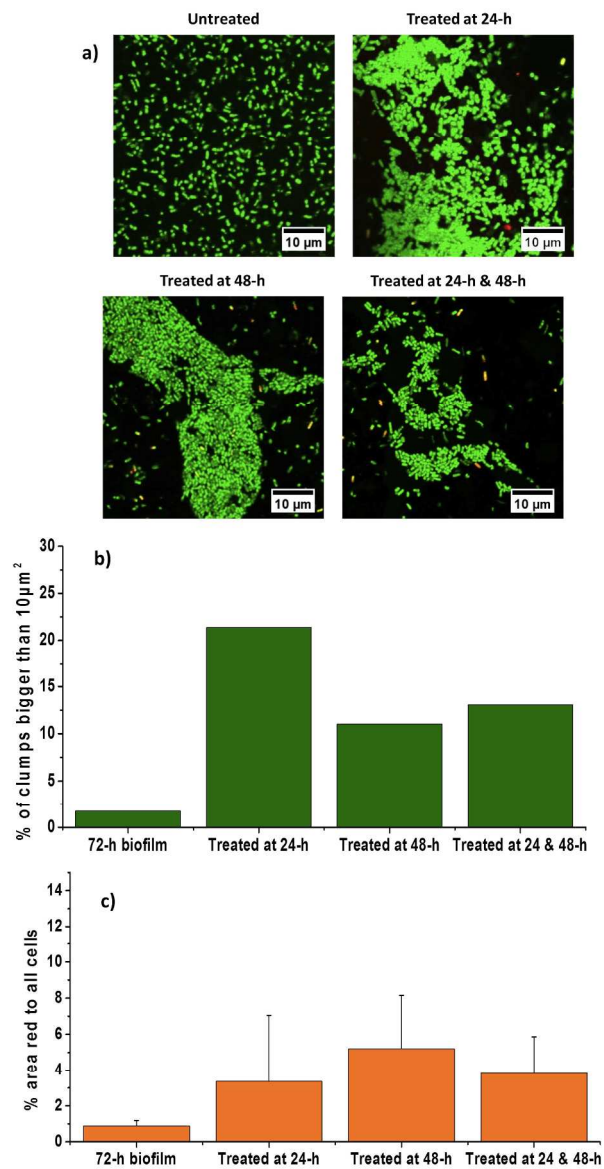
Figure 4. a) Confocal images of untreated 72-h biofilm and biofilm grown for 72-h but exposed to 30s plasma treatment at different biofilm ages, where it is shown that biofilms retain their aggregated structure after those plasma treatments, b) percentage of clumps bigger than 10µm2, c) quantification of red cells

330x505mm (300 x 300 DPI)
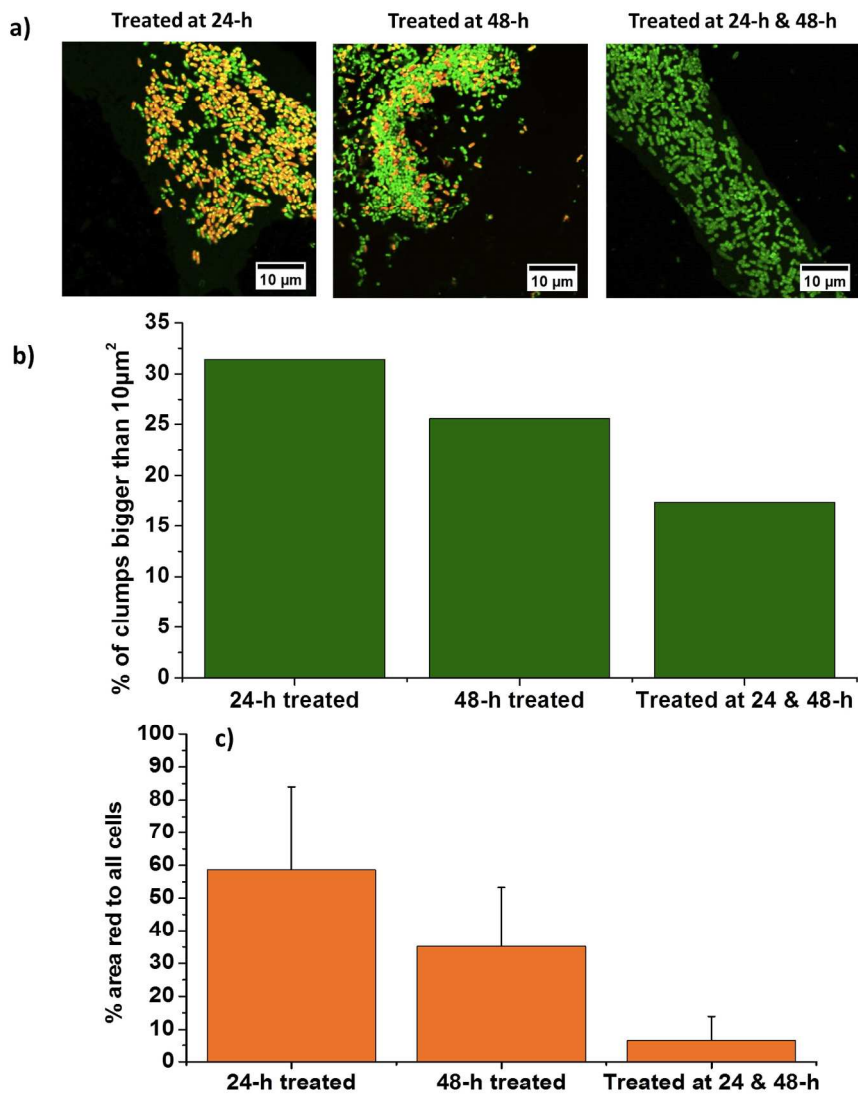
Figure 5. a) Confocal imaging of plasma-treated samples that were imaged right after treatment where less cells are killed after treated twice, b) the percentage of aggregates bigger than 10 µm2, c) quantification of dead cells

314x358mm (300 x 300 DPI)
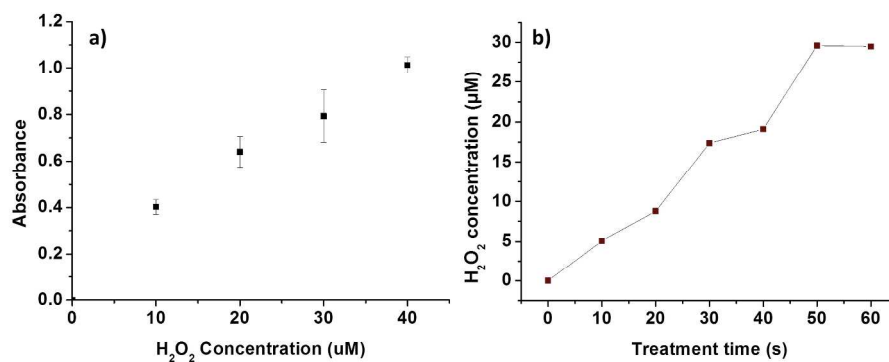
Figure 6. a) Calibration curve for H2O2 by spectrometer at 610nm, b) The H2O2 concentration in plasma-treated liquid.

469x182mm (300 x 300 DPI)
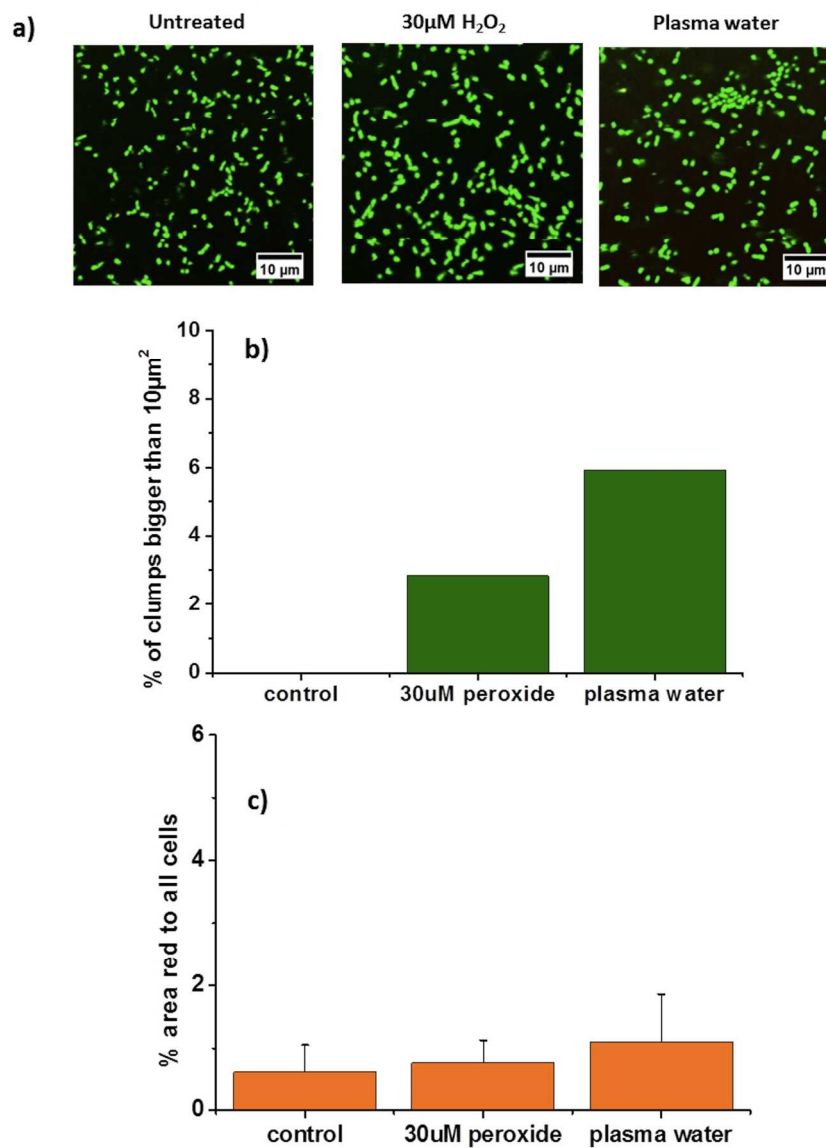
Figure 7. a) Confocal images of untreated biofilm, incubated with 30µM H2O2 and incubated with plasma liquid treated for 60s, b) percentage of aggregates bigger than 10 µm2, c) red cells quantification of samples

144x199mm (300 x 300 DPI)
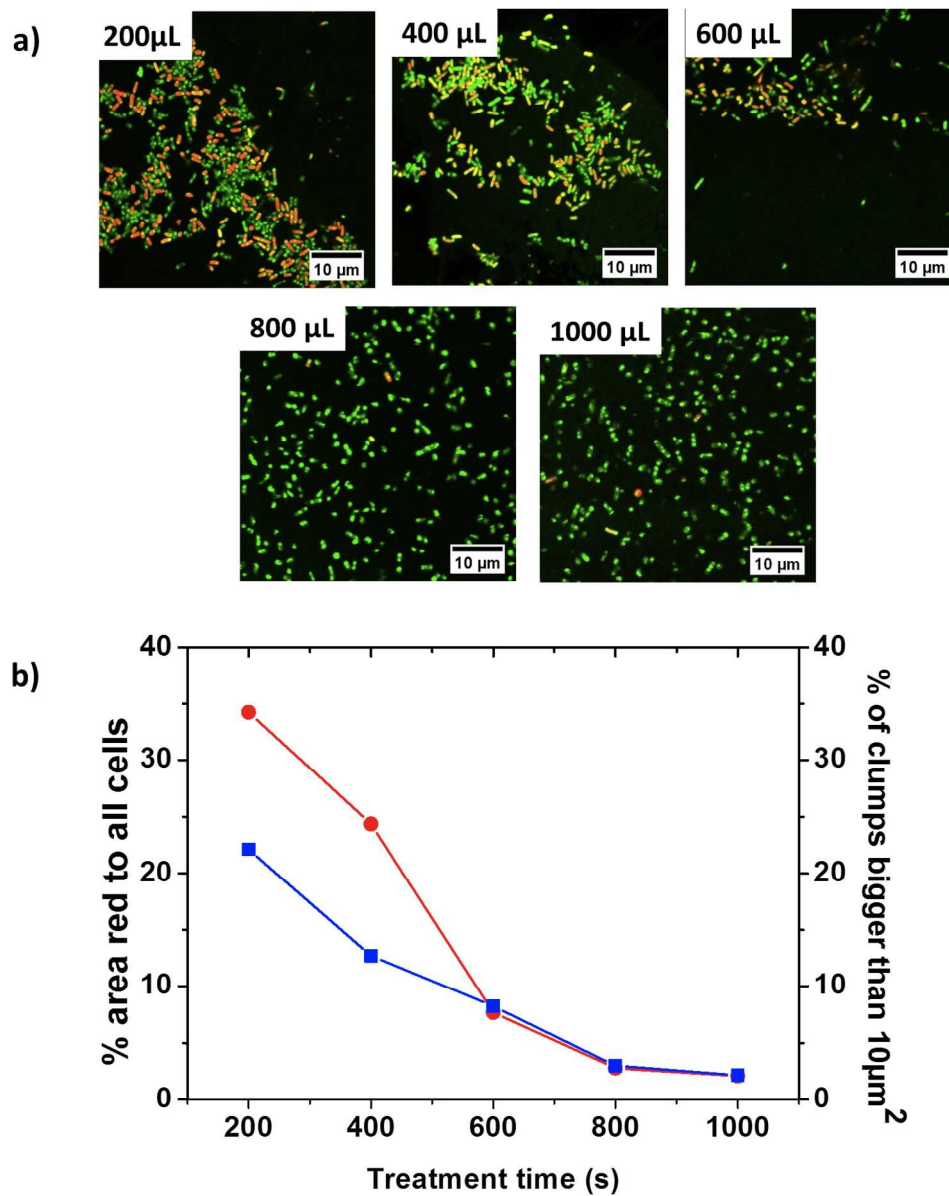
Figure 8. The effect of liquid volume covering biofilm during plasma treatment on aggregation and cell death a) confocal images of different structures observed, b) quantification of dead cells (symbol ●) and cell clumps larger than 10µm2 (symbol)

263x326mm (300 x 300 DPI)
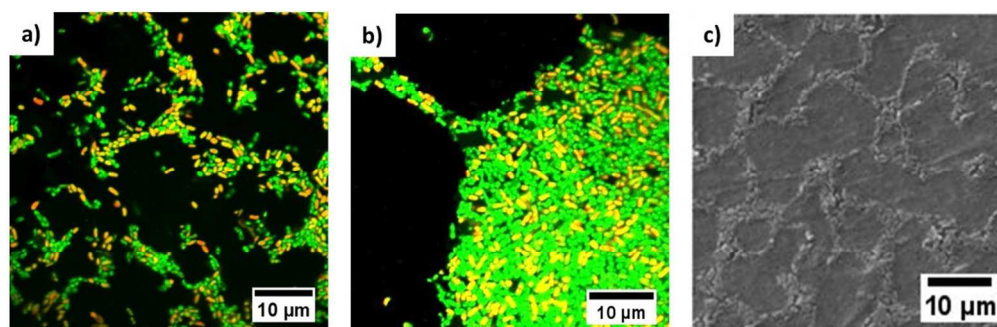
Figure 9. a) Circular pattern ring structure formed by bacteria after plasma treatment, b) Compact structure formed by bacteria after plasma treatment, c) Redrawn pattern rings formed by surface-deposited bacteria after plasma treatment observed by Bayliss et al[29]

309x99mm (110 x 110 DPI)
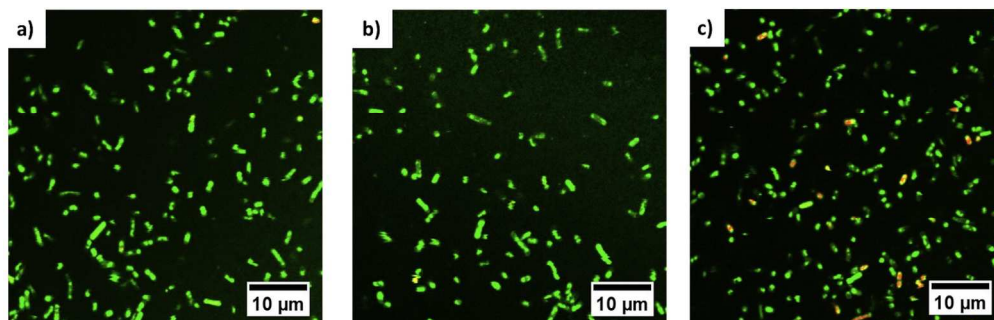
Figure 10. The drying effect on structure of biofilm by oven at 50°C for different treatment time. a) treated for 30 s, b) treated for 60 s, c) treated for 90 s

254x80mm (300 x 300 DPI)